Correlation of CZCS Surface *k*s with *k*s Derived from Secchi Disk*

Abstract

As part of a validation procedure for Coastal Zone Color Scanner (CZCS) determined downwelling diffuse attenuation coefficients, or k values, Secchi disk derived ks were compared to CZCS computed ks. The preliminary results of such a comparison exhibited that the Secchi derived ks were consistently higher than the CZCS ks. The objective of this writing is to explore the reasons for this discrepancy and suggest causes to explain and interpret these results.

Background

The Coastal Zone Color Scanner (CZCS), algorithm for determining the downwelling irradiance coefficient, or *k*, for Case 1 waters uses the upwelling radiance from the 443-nm and 550-nm bands. The algorithm for *k* at 490 nm has the form (Austin and Petzold, 1981)

$$k(490) = 0.0883 * \left[\frac{L_u(443)}{L_u(550)}\right]^{-1.491} + 0.022 \qquad (1)$$

where $L_u(443)$ and $L_u(550)$ are the upwelling radiance in the 443 and 550 channel, respectively. The algorithm was devised using *in situ* measurements from a variety of sources. Using a regression analysis on the datasets, Equation 1 was obtained at a correlation coefficient value of $r^2 = 0.901$. Because the algorithm was developed using *in situ* data and the radiances observed by a spaceborne sensor are primarily (up to 80 percent to 90 percent of received radiance) due to atmospheric scattering (Gordon, 1990), the corrections for the atmospheric contributions to the received signal become critical and are the largest contributor to error in the computation of *k*s in a CZCS image for the 1979 CZCS data used in this work. Later in the lifetime of the sensor, calibration issues became a problem which led to the emergence of another large error component in the data.

Secchi disks have had a long and venerable history in hydrologic optics (Preisendorfer, 1986). Large Secchi disk databases exist from the past century to the present. These data, if treated as purely optical data, represent the largest repository of information concerning the water optics of natural waters. A Secchi disk represents an inexpensive and simple to use oceanographic tool. The usual procedure for taking a Secchi disk measurement is to lower the disk into the water on the sunny side of the ship. Record the depth where one can just make out the disk. Record the depth where the disk just disappears. Take the average of the two readings and document this as the Secchi depth, Z_s.

Diffuse attenuation coefficient, or *k*, values are not directly obtainable from Secchi depths (Pilgrim, 1984). Seeing the Secchi disk at a given depth or not seeing the disk at a given depth is a problem of visibility, or contrast. Hence, the observation of a Secchi disk becomes more of an issue of the propagation of contrast through natural waters (Tyler, 1968) rather than that of simply the up or downwelling radiances alone. The Duntley-Preisendorfer relation for the propagation of contrast is given by the form (Preisendorfer, 1986)

$$C_z = C_o \exp(-(k + c)Z) \qquad (2)$$

where C_z and C_o are the apparent and inherent contrasts (Duntley, 1952), *c* is the beam attenuation coefficient (Gordon *et al.*, 1984), and *Z* is the depth.

The $k+c$ term in Equation 2 is critical to understanding the limitations of Secchi disk information. The *k* is the appropriate attenuation coefficient for the illumination of the disk at depth *Z*. The beam attenuation coefficient, *c*, is the appropriate attenuation coefficient for the imaging of the disk by the human eye. Thus, the $k+c$ term represents a two-way attenuation coefficient for the downwelling (which illuminates the water and disk) and the upwelling (which, ultimately, allows the act of observation to take place) light fields.

The $k+c$ term cannot be broken into its components without supplementary information about the optics of the water mass in question. Normally, the additional information about the water necessary to break apart the *k* and *c* terms requires more sophisticated measurements which, in effect, displace the Secchi disk measurements themselves. Hence, these days, most optical oceanographers dispense with making Secchi disk measurements and concentrate solely on radiometric measurements made with more elaborate electronic instrumentation.

However, because of the large historical database, and the ease with which a Secchi disk measurement can be made, the use of the Secchi disk continues as does the search for ways to utilize the optical information embedded in the compiled database. In order to derive *k*s from Secchi depth information, simultaneous measurements of *k* must be made with Secchi depth measurements. A regression analysis can then be used to map Secchi depth to *k*. The regression relations often take the hyperbolic form

$$k = \frac{\text{Constant}}{X_s} + \text{Correction Term} \qquad (3)$$

where the Constant factor can vary quite widely, and the Correction Term often represents a relatively small number (Preisendorfer, 1986).

Nonetheless, in the attempt to map visibility of the disk to only the attenuation of the illumination field of the disk, an oversimplification of the problem has occurred. This usu-

*Presented at the First Thematic Conference on Remote Sensing for Marine and Coastal Environments, New Orleans, Louisiana, 15–17 June 1992.

L. Estep and **R. Arnone**
Naval Research Laboratory, Stennis Space Center, MS 39529

Photogrammetric Engineering & Remote Sensing,
Vol. 59, No. 3, March 1993, pp. 345–350.

0099-1112/93/5903–345$03.00/0

ally means that the empirical relationship represented by the regression function will break down quite easily if the optical circumstances shift somewhat. Thus, the Z_s to k mapping will be profoundly affected by seasonal changes, local currents (or other hydrodynamic phenomena), and geographical location. This means that the mapping found is usually good only for the locale and season for which it was originally calculated. Presently, not much is known about temporal or spatial optical variability (vertical or horizontal) for ocean waters. Therefore, it is quite difficult to say how "local" some of the mappings are. Suffice it to say, such relations are best kept "near home" and used in the appropriate time of year.

Discussion of Date Sources and Initial Correlation Problems

The CZCS historical data source for the validation effort came from the Navel Research Laboratory (NRL), Mapping, Charting, and Geodesy Division. Level 2 processed CZCS data were obtained from the NASA Goddard facility. These data were processed to derive the surface k values at 490 nm over the entire scene imaged by the CZCS sensor (R. Arnone, personal communication, 1991). The atmospheric correction to the scene has been already applied as part of the level 2 processing effort by Goddard prior to shipping the scene to NRL.

The primary source of Secchi disk data used in the validation effort came from the National Oceanographic Data Center (NODC). The NODC maintains a Worldwide Ocean-Water Color/Water Transparency database which is available from the National Oceanographic and Atmospheric Administration (NOAA) (Hollman and Weideman, 1989). The Secchi depths documented in the database were partitioned into eight primary geographic areas around the continental United States. The data were sieved to remove bias from too frequent coastal measurements, and converted to k values using empirical relationships of the kind generalized in Equation 3 (Hollman and Weidemann, 1989). The eight primary areas were further subdivided into rectangular regions. Using what was considered to be appropriate Z_s to k conversions for an area, the resulting k values calculated were averaged to yield the appropriate k value for the particular regions in an area. It is usually assumed that the k values are

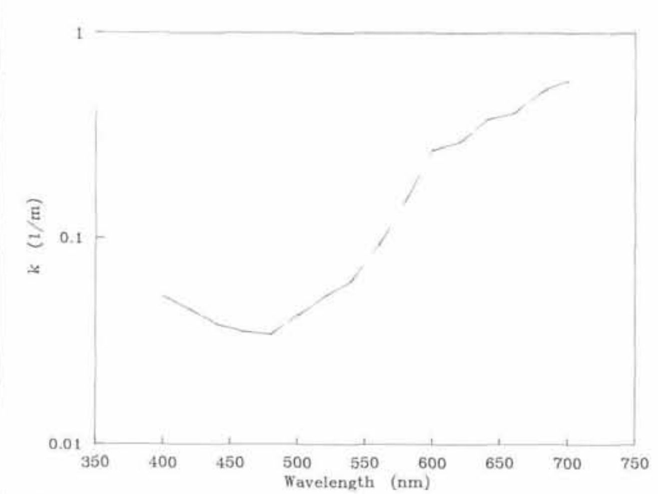

Figure 2. Spectral k attenuation curve for Jerlov type IB water masses.

computed at 550 nm which is practically identical to the peak of the spectral eye response curve (Williams, 1970).

Figure 1 shows a sample plot of the data for the northwest Atlantic area. The diagonal line drawn in the plot represents the identity function or a line of perfect correlation. The two points that mark the starting point and terminus of the line are not data points. They are used to enable the drawing of the line itself. The data are plotted without regard to wavelength differences in the two datasets. The plot shows that, ostensibly, the Secchi disk measures "dirtier" water than the CZCS sensor.

Figure 2 shows a typical Jerlov water type curve (Jerlov, 1976). This curve exhibits the k values for Jerlov Class IB water. The minimum attenuation suffered by light in traversal of such a water mass is close to the CZCS 490-nm value. However, as one moves to the 550-nm value, the K value increases. Therefore, in Figure 1, part of the dis-correlation of the two ks plotted comes simply from the ks not being at the same wavelength.

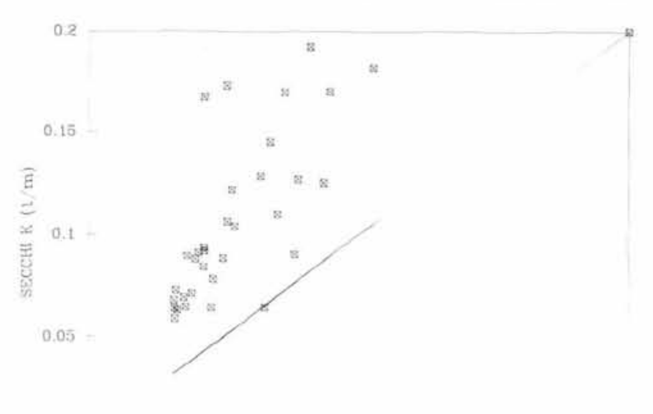

Figure 1. CZCS ks (490 nm) versus Secchi ks (550 nm) for northeast Atlantic area.

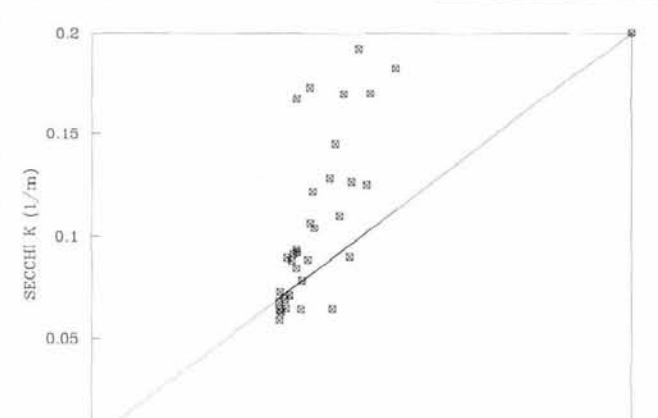

Figure 3. CZCS ks corrected to 550 nm versus Secchi ks at 550 nm.

Figure 3 shows the northwest Atlantic plot again but with the CZCZ values recomputed for equivalent 550-nm values. The dis-correlation of the two *k* datasets is still equivalent.

Analysis and Discussion

The observation of the ocean's upwelling radiances by the CZCS sensor system was done for specific channels, or wavelength bands. The bandwidths of the CZCS visible channels were ± 10 nm (Hovis, 1981). That is, light of a specific color was passed while all other colors of light were rejected. Therefore, specific radiance streams were seen by the sensor and used in the post processing of the data.

The observation of the Secchi disk by the photopic human eye is broad-banded. The human eye frequency response goes across the visible spectrum but is not equally sensitive at every color.

Figure 4 shows the human (photopic) eye spectral response curve (Boyd, 1983). The peak of the curve comes at about 550 nm. Hence, Secchi disk observations are often assumed to have applicability at this wavelength. However, in looking at Figure 2, it can be seen that the attenuation by the water for the 550-nm wavelength is much greater than that at the "bluer" wavelengths. Hence, the 550-nm wavelength can be filtered by the water column, depending on water type, so that very little or no light at that wavelength is available for the eye to see.

It is evident that the photopic eye and the water mass are an optical system which act in concert when viewing a Secchi disk. Thus, the eye-water system spectral response curve must be determined to find the peak wavelength passed by the system. It is this wavelength that is used by the eye to make an observation of the disk at depth. That is, the peak wavelength provides the deepest observation of the Secchi disk – which is defined as the Secchi depth.

Figure 5 shows the spectral response curve of the eye-water system for Jerlov IB water. The peak of the curve comes at 510 nm. Hence, the Secchi *k*s need to be corrected from the 550-nm values stated originally to 510-nm values. Similarly, the CZCS 490-nm values must be shifted to 510 nm to compare with the Secchi derived ks.

Assuming Jerlov IB waters hold for the northwest Atlantic area, Figure 6 shows that same data as in Figures 1 and 3 but now both the CZCS and Secchi *k*s are at 510 nm. Although there is some scatter still evident, the correlation seen between the two data sets is much improved. The center of mass of the data lies quite near to or on the identity function line, or line of perfect correlation.

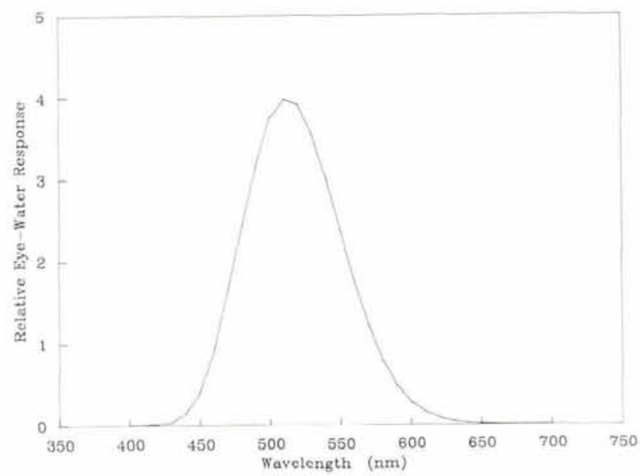

Figure 5. Faltung results of the photopic eye spectral response curve with Jerlov IB waters.

Perhaps a better way to look at the data is to develop a correlation plot which allows one to see more clearly the variation of the data and the correlation of the data, data point by data point. The first step is to form the ratio of a Secchi *k* to the CZCS *k* for a datapoint and subtract unity. This was done for every point in the scatter plot of a region.

If the Secchi and CZCS *k*s were perfectly correlated for that region, they would lie along the line $y=0$. The dataset is now replotted where the ordinate values are the ratioed *k*s and the abscissa represents the number of the paired *k* observations.

Figure 7 shows a "correlation plot" of the dataset of Figure 6. The excursion distance of a data point from the $y=0$ line is the measure of correlation of that point in the plot. The smaller the distance, the better the correlation. The dis-

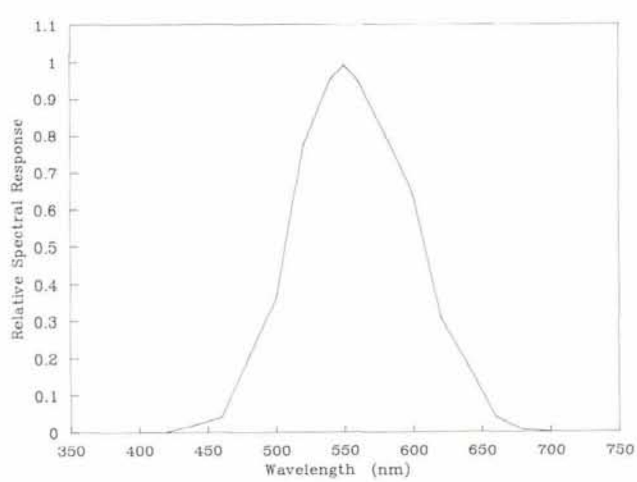

Figure 4. Spectral response of the photopic human eye.

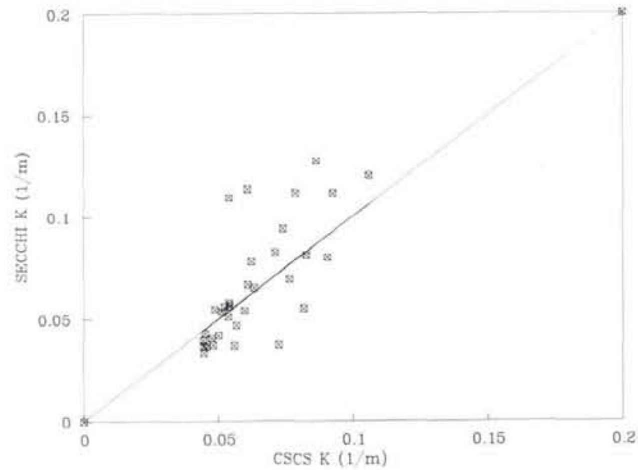

Figure 6. CZCS and Secchi derived *k*s both moved to 510 nm.

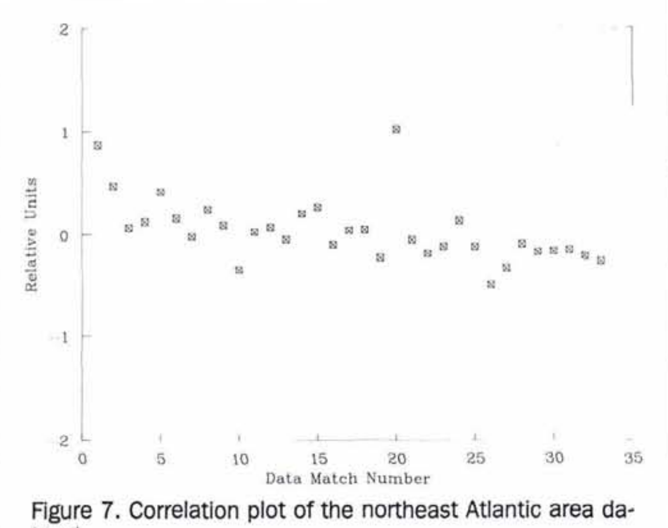

Figure 7. Correlation plot of the northeast Atlantic area dataset.

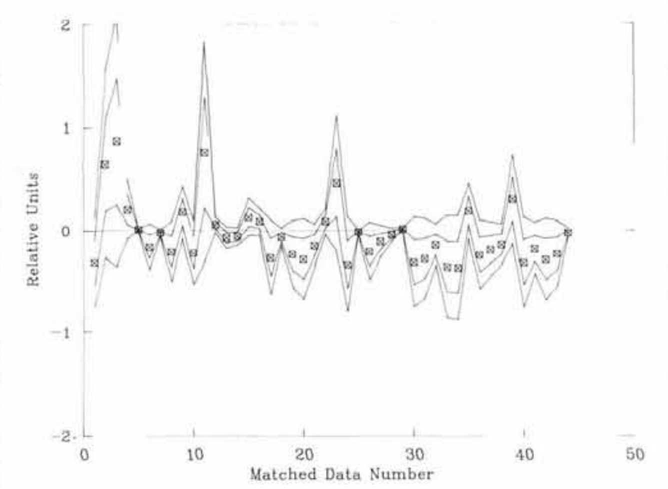

Figure 9. Correlation plot of the Gulf of Mexico.

tance above or below the identity function line is simply given by the y values themselves. Assuming Gaussian statistics, and independent errors in the CZCS ks and Secchi ks, the errors in the CZCS ks and the Secchi derived Ks can be propagated through the ratioing of the two k datasets. The results can be charted on the above correlation plot as lines above and below the points shown. Figure 8 shows an example. The two sets of lines in the plot give error bands of 50 percent and 100 percent about the data points. To interpret the graph, locate a datapoint and an error band of interest; if the error band containing the point also contains the line $y=0$, then the CZCS and Secchi k values are correlated at that point. It is seen that all the points are correlated at the 100 percent error level.

Figures 9 and 10 show similar graphs of the Gulf of Mexico and Northwest Coast areas.

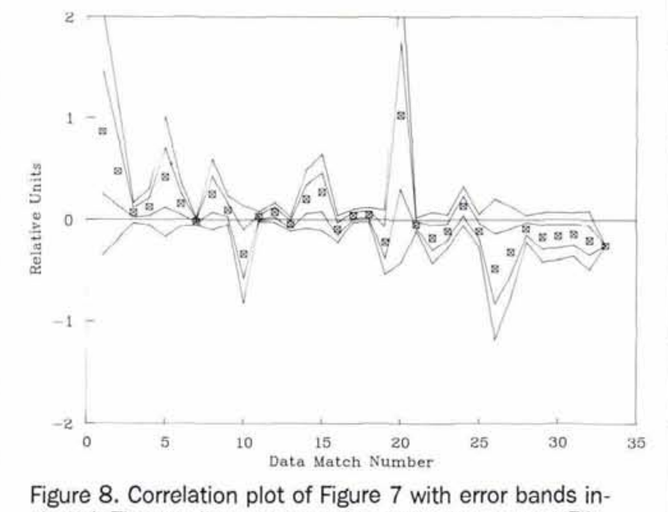

Figure 8. Correlation plot of Figure 7 with error bands included. The two lines nearest the x-axis represent a 50 percent error band. The two lines farther away represent a 100 percent error band.

Error Sources and Magnitudes

In the graphs shown, three categories of deviations from perfect correlation are evidenced. The first category is the displacement of the DC level of the data from the $y=0$ identity line. The second category is apparent trends of the datasets with reference to the $y=0$ line. The third category is represented by the scatter of the data about the centroid of the dataset. For example, for the first category aforementioned, the DC offset for Figure 9, the Gulf of Mexico region, is slightly below the $y=0$ line. The DC offset is slightly above the line for the Northwest Coast area (Figure 10). It should be noted that the CZCS ks and Secchi derived ks in Figure 10 were corrected for 540 nm. By comparison, Figure 8, the Northwest Atlantic, shows little DC offset. However, Figure 8 shows an example of an apparent trend from higher than the $y=0$ line on the left to lower than the $y=0$ line on the right. All of the plots exhibit some scatter of the data.

The first category of deviations, as defined above, is a DC offset from the $y=0$ line. Deviations such as these can be due to inappropriate Secchi relationships that derive k from

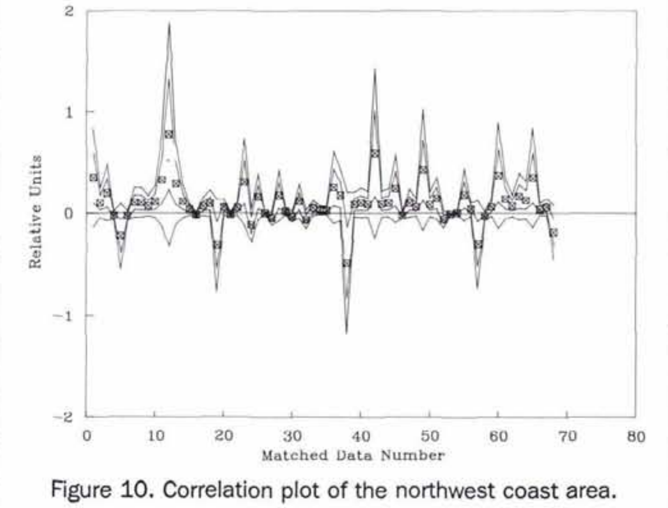

Figure 10. Correlation plot of the northwest coast area.

the Secchi depth, water masses which are more turbid and affect the atmospheric correction algorithm of the CZCS sensor, and that the convolution of the eye and water response curves lies not quite at the wavelength stated in the plot. Secchi relationships can be quite varied (Pilgrim, 1984).

Table 1 gives a listing of the relationships often used in computing k from Secchi Depth and Figure 11 gives a plot of a few of these relationships.

Hojerslev (1986) states that Graham found values of the constant, C, to range from 0.3 to 1.6 in the northeastern Pacific. Such findings have led to the conclusion that C cannot be constant for all water types (Nielsen, 1985). Hojerslev gives the relation $3.3/Z_s$ based on the elimination of c from the propagation of contrast equation using a k to c relationship given by Timofeyeva (1974). There are several of these sorts of k to c relations in the literature (Shannon, 1975; Phillips *et al.*, 1984) based on empirical relationships derived from field datasets wherein both k and c were measured simultaneously. This in another path sometimes taken by researchers to derive a Secchi depth to k relationship.

This approach is fraught with dangers because k documents an apparent optical property of the water mass and c an inherent optical property (Preisendorfer, 1976). Because of this, there can be no universal relationship between k and c – only local ones. Moreover, Timofeyeva derived his relationship in a laboratory situation using "milky" media, or very turbid aqueous solutions. The k most applicable in these laboratory conditions is the asymptotic k value (Preisendorfer, 1976). Generally speaking, the asymptotic k is not the average k that will apply for the near surface waters wherein the Secchi disk observation is being made.

Each of the above relations between Z_s and k has been derived for datasets of some particular location. For example, Poole and Atkin's (1929) relationship was derived for the waters of the English Channel. The specific area of the channel or season of the year the relationship is valid for is not given. This is generally true for these relationships. No consideration for the spatial and temporal variability of the water mass is given, albeit such variability is widely accepted.

Therefore, confronted with a large Secchi depth databases and the need to derive useful optical information in the form of k values, the researcher generally succumbs to using relationships such as those discussed. However, it will be difficult to know which relationship to use in a given region. Averaging over k derived from such relationships smooths the results but does not assure greater accuracy because the basic relationships are in doubt. It is very difficult to know what error bounds to put on the results once the computations are completed.

Given all that has been documented about the Secchi depth to k relationships, a large error is logically expected. As an aid to obtaining a feeling for the possible error, k data used from the Key West area were compared to Secchi depth derived k values in Figure 12. The error curve in Figure 12 has been divided by 10 so that is could be plotted simultaneously. The point by point error ranges from 66 percent to 100 percent. However, in view of what has been said, this in in line with what one would expect from such relationships applied to water masses different from those wherein the relationships were first derived.

TABLE 1. SECCHI DEPTH TO K RELATIONS.

Source	Relation: $k=C/Z_s$
Poole and Atkins (1929)	$k=1.7/Z_s$
Weinberg (1976)	$k=1.39/Z_z$
Quasim (1968)	$k=1.5/Z_s$
Holmes (1970)	$k=1.44/Z_s$
Cooper and Milne (1938)	$k=1.59/Z_s$
Nielsen (1966)	$k=1.85/Z_s$
Graham	$k=0.3/Z_s$

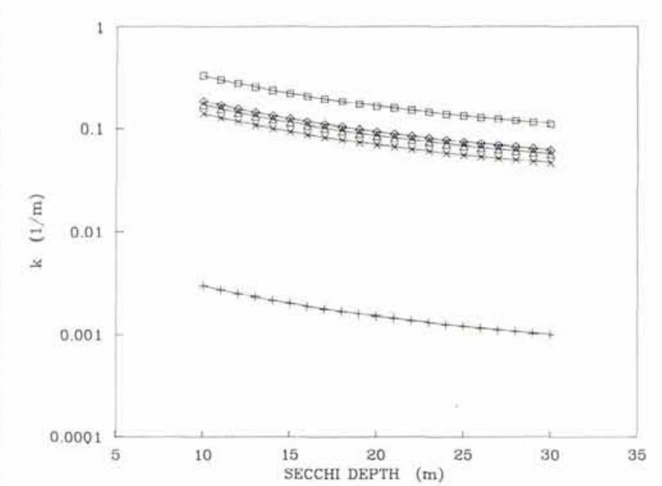

Figure 11. Plots of Z_s to k relationships.

The DC offset due to errors in the CZCS data can now be considered. The k values are computed pixel by pixel over the scene of interest. The swath width of the CZCS sensor was 1636 km and the usual processed (Level 2) pixel size was 18 km^2. The atmospheric correction applied to the CZCS data is usually acknowledged as the source of greatest error in the k computations for data acquired before significant aging of the sensor occurred. Moreover, the atmospheric correction that was applied to the image was a "blanket" correction using a constant value of zero (maritime atmosphere) for the Angstrom coefficient (R. Arnone, personal communication, 1992) which could be erroneous for certain images and, also, would not take into consideration sub-regions in the image where atmospheric conditions could be different from other sub-regions. Errors of this sort in the at-

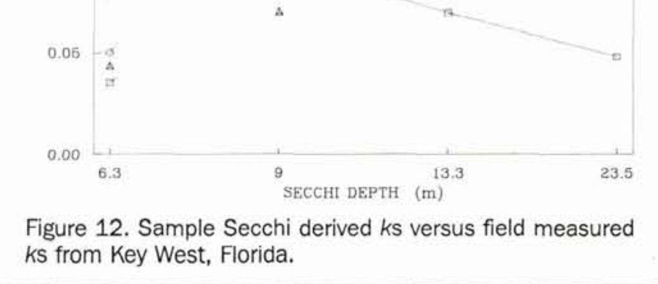

Figure 12. Sample Secchi derived *k*s versus field measured *k*s from Key West, Florida.

mospheric correction no doubt occurred. The size of the errors for the atmospheric correction have been estimated to be 100 percent (Hickman *et al.*, 1991).

In Figures 7, 8, and 9, the assumption has been made that the water body approximated the Jerlov Type IB water mass. However, this is a guess. In maps which show the central Jerlov water mass type of many of the areas of interest, Jerlov IB dominated. However, this amounts to employing some coarse averaging of the optical characteristics actually present over the course of a year. Hence, it is possible that the water mass is not "pigeon-holed" properly by the Jerlov IB assumption, and the convolution of the spectral eye response with some slightly different water filter response is needed for the correction of the *k*s. For example, Figure 10 exhibits data for the Northwest Coast region. Here, the *k*s were corrected to a wavelength of 540 nm to obtain the correlation plot seen.

The trends alluded to in Figure 8 of the Northwest Atlantic region can be interpreted as seasonal effects which became manifest in the data when plotted in the correlation plot format. The composite plot of all seasons in Figure 8 runs from Winter points on the left to Fall points on the right. Thus, it appears that the seasonal optical character of the water mass deviates enough to impact either the Secchi disk relationships used in the *k* calculation and/or the atmospheric correction for the CZCS. Thus, the water mass appeared to be approximating a Jerlov Type IB water class in Spring and Summer but deviating slightly from it in the Winter and Fall.

Scatter evident in the data can be understood by considering the problems of taking point measurements, as in Secchi disk observations, and comparing them to monthly averages over an image pixel. The size of the CZCS pixels was 18 km². With this size of picture element, the spatial variability over the corresponding area could be significant. Moreover, while the CZCS *k* gave a monthly average over 18 km², a Secchi *k* gave a *k* value at a small sub-region in the pixel at a specific time. Consequently, simple statistical variation in the value of *k* within the CZCS pixels is expected and might account for some of the comparative scatter in the data.

Conclusions

The original problem addressed was the lack of correlation between the Secchi depth derived *k*s and the CZCS computed *k*s for all the regions studied. The problem was resolved by considering the eye and specific water mass as an optical system through which the Secci disk observation is made. This provided a spectral response curve for the eye-water system. The spectral response curve provided a peak response for the system to which both the Secchi *k* and CZCS *k* must be corrected. These corrected *k* values were then plotted on a correlation plot and analyzed in terms of the sources and magnitudes of the errors that arise. It is shown that the errors are large enough in both the Secchi and CZCS methods of deriving *k*s that the points fall within the appropriate error bands in the correlation plots. This means, within the errors documented, the Secchi and CZCS derived *k*s were presumed to be correlated.

References

Austin, R.W., and T.J. Petzold, 1981. The determination of the diffuse attenuation coefficient of sea water using the Coastal Zone Color Scanner. *Oceanography from Space* (J.R.R. Gower, editor), Plenum Publishing, London, 13:239–256.

Boyd, R.W., 1983. *Radiometry and Detection of Optical Radiation*. J. Wiley & Sons, New York, N.Y.

Duntley, S.Q., 1952. *The Visibility of Submerged Objects*. Visibility Laboratory, MIT, Cambridge, Massachusetts, 74p.

Gordon H.R., 1990. Radiometric considerations for ocean color remote sensors. *App. Opt.*, 29:3228–3236.

Gordon, H.R., R.C. Smith, and J.R. Zaneveld, 1984. Introduction to ocean optics. *Ocean Opt. VI., Proc. SPIE*, 489:15–55.

Hickman, G.D., S.C. Gallegos, and M.J. Duggin, 1991. *Accuracy of Ocean Color Data Derived from the Coastal Zone Color Scanner (CZCS)*. Naval Oceanographic and Atmospheric Research Laboratory, TN–116, Stennis Space Center, Mississippi.

Hojerslev, N.K., 1986. Visibility of the sea with special reference to the secchi disk. *Ocean Opt. VIII, Proc. SPIE*, 637:294–305.

Hollman, R., and A. Weidemann, 1989. *Secchi Depth Data Base*. Naval Ocean Research and Development Activity, TN–456, Stennis Space Center, Mississippi.

Hovis, W.A., 1981. The Nimbus–7 coastal zone color scanner (CZCS) program. *Oceanography from Space* (J.R.R. Gower, editor), Plenum Publishing Co, London.

Jerlov, N.G., 1976. *Marine Optics*. Elsevier Publishing, New York.

Nielsen, S., 1975. *Marine Photosynthesis*. Elsevier Publishing, New York.

Phillips, D.M., R.H. Abbot, and M.F. Penny, 1984. Remote sensing of sea water turbidity with an airborne laser system. *Journ. of Appl. Physics*, 17:1749–1758.

Pilgrim, O.A., 1984. The Secchi disk in principal and use. *Hydrog. Journal*, 33, pp. 25–30.

Preisendorfer, R.W., 1976. *Hydrologic Optics*. Vol. 1., U.S. Dept. of Commerce, USPGO, 1976–678–487/56 Region 8, Washington, D.C.

———, 1986. *Eyeball Optics of Natural Waters: Secchi Disk Science*. NOAA Memorandum ERL PMEL–67, Washington, D.C.

Shannon, J.G., 1975. Correlation of beam and diffuse attenuation coefficients measured in selected ocean waters. *Ocean Opt. VII, Proc. SPIE*, 64.

Timofeyeva, V.A., 1974. Optics of turbid waters. *Optical Aspects of Oceanography*. Academic Press, New York. pp. 177–218.

Tyler, J.E., 1968. The Secchi disk. *Limnol. and Oceanog.*, 13:1–6.

Williams, J., 1970. *Optical Properties of the Sea*. U.S. Naval Institute, Anapolis, Maryland.